AGH Journal of Mining and Geoengineering • Vol. 36 • No. 2 • 2012

Ewa Kawalec-Latała *

DETECTION OF SELTS DEPOSITS GEOMETRY VARIATION

1. Introduction

Most underground hydrocarbon storage facilities are located in depleted natural gas reservoirs. Much more efficient reservoirs are those constructed in rocky salt. Their placement could be in the salt dome, but better localisations due to less complicated geological conditions are to be found in salt deposits. Salt deposits are one of the important potential places for underground reservoirs. Rock salt has the following properties: chemical interia, very low permeability In Poland there are favourable conditions for the construction of such storage in thick-bedded salt of high homogeneity [4]. The thickness of rock salt varies. An area of extremely high thickness (over 100 m) of salt is the most convenient location for underground reservoirs of liquid fuels as well as underground storage of waste. The safe storage of highly radioactive waste (HWL) is very problematic [5, 6]. Also the sequestration of CO_2 to underground reservoirs will reduce its emission to the atmosphere.

The internal structure of salt deposit displays several lithological types of rock salt (pure coarse-crystalline salt, anhydrite salt, salt intercalated with anhydrite). The thorough examination of inhomogeneities within salt deposits became especially important. Geometrical variations as well as chemical and physical properties of salt deposits have to be a subject of careful examination. Particularly important for the construction of underground reservoirs is the homogeneity of large parts of deposit.

Rock mass containing salt deposits display high seismologic inhomogeneity. Due to the considerable contrast of elastic properties of salt versus neighbouring layers within the Zechstein rocks high reflection coefficients are observed. Inhomogeneities in a geometrical sense are related to thickness changes, dying-out of strata and the presence of lenses. Geometrical changes depend on the sedimentary processes as well as on those later alterations within rocks

* AGH University of Science and Technology, Faculty of Geology, Geophysics and Environment Protection, Department of Geophysics, Krakow

salt deposits, which in turn lead to the origin of secondary, descendant salts. The detection of anhydrite salt occurring in the neighbourhood of rock salt is necessary. The work concerns the possibility of the recognition of the space distribution of anhydrites in the rock salt.

A method of inversion of a seismic section aiming at obtaining a pseudo-acoustic impedance section gives the possibility to very closely bind the acoustic impedance changes with lithologic and facial changes in subsurface. Seismic traces are converted first into pseudoreflection coefficient time series, then into acoustic impedance by the inversion of the time series. The basic concept is simple; a reversal of the procedure long used to compute synthetic seismograms from sonic logs. In practice the reverse process is difficult, since it requires inversion of a low grade, the seismic trace, which is often, distorted by noise and wave propagation phenomena, into the higher-grade sonic log signal.

Modern seismic field data can be processed to eliminate much of the distortion. An important procedure to help repair the damage to the spectrum (caused by seismic source, transmission trough the earth and the recording instruments) is deconvolution.

2. Results — modelling example

Many technical problems connect with inter-calculations of anhydrite in the deposits of Zechstein evaporates within rock salt beds. Their presence have been taken into account for creating the theoretical models in order to test the possibility to detect its distribution in sections of pseudoacoustic impedance. Three theoretical, simplifying models have been constructed figures 1, 2, 3. The top of the rock salt on all models is on 300 m and the bottom on 450 m.

Model I is related to thickness changes due to dying-out of strata of anhydrite. The thickness of anhydrite change from 40 to 0 m at the left side, and from 30 to 0 m at the right side, figure 1.

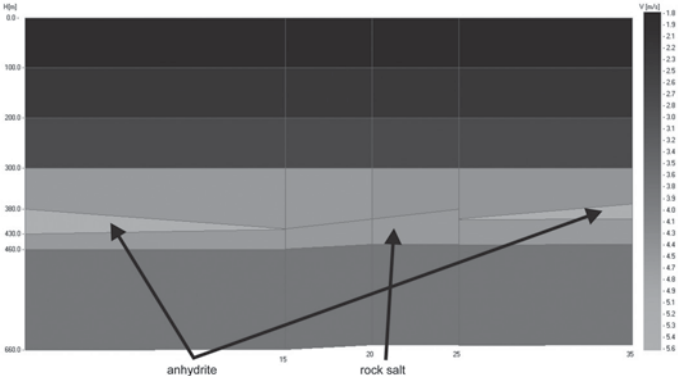

Fig. 1. Simplified seismological model I. Left Vertical axe depth in meters, horizontal axe: number of traces, right axe: wave velocity in m/s displayed as colour scale

The model II and model III are related with presence of anhydrite lenses. The big lens of thickness between 0–100 m and small one of thickness between 0–50 m are presented in figure 2 and 3, respectively.

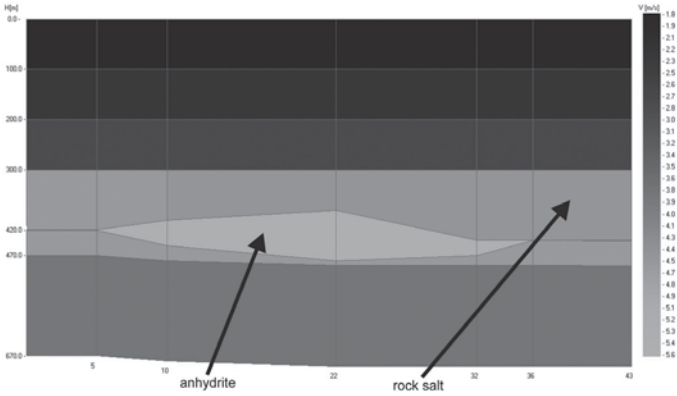

Fig. 2. Simplified seismological model II. Left Vertical axe depth in meters, horizontal axe: number of traces, right axe: wave velocity in m/s displayed as colour scale

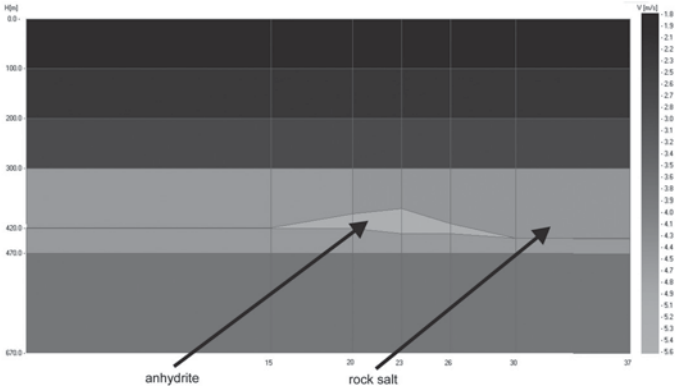

Fig. 3. Simplified seismological model III. Left Vertical axe depth in meters, horizontal axe: number of traces, right axe: wave velocity in m/s displayed as colour scale

The synthetic pseudoimpedance acoustic sections are generated for the simplified data. These are obtained by the inversion process based on recursive relation. There are several ways to achieve this objective [7]. It should be realised that the inversion procedure is not a unique process. There is no single solution to any given problem. Feasibility studies with synthetic modelling are recommended. For the modelling of pseudoimpedance sections a computer system INVERSE [3] was used. The system INVERSE consist of two main parts:

1) modelling
2) visualisation of results.

The modelling takes two steps. First the synthetic seismogram was calculated as a convolution of reflection coefficient series with seismic signal. Next the process inversion is made Seismic traces are converted into pseudoimpedance traces. The synthetic seismogram was calculated as a convolution of reflection coefficient series with seismic signal. The signal of Puzyriev $s(t)$ was applied:

$$s(t) = \exp(-\beta^2 \cdot t^2) \cdot \sin(2\pi \cdot f_0 \cdot t \pm \varphi_0) \tag{1}$$

The parameters of signal are: f_0 — dominant frequency, φ_0 — initial phase, β — dumping factor.

The ratio f_0/β determine the length of signal. When the ratio is 1 the signal is relatively short, the ratio 2 gives the long signal.

A number of synthetic pseudo-acoustic impedance sections were constructed. for simplified models presented in figures 1, 2, 3. The rock salt on synthetic pseudoimpedance acoustic sections is observed in time limit between 0.27–0.33s (300 m and 450 m respectively on the geological model). The colour scale reflecting the relative velocity (or acoustic impedance) variations, was added at the right side.

The synthetic pseudoimpedance acoustics section presented in figures 4, 5, 6 are generated for simplified model I presented in figure 1. The sections are generated for dominant frequency f_0 = 60Hz. The synthetic pseudoimpedance acoustics section generated for short signal duration time f_0/β = 1 (f_0 — dominant frequency, β — dumping factor), is presented in figure 4.

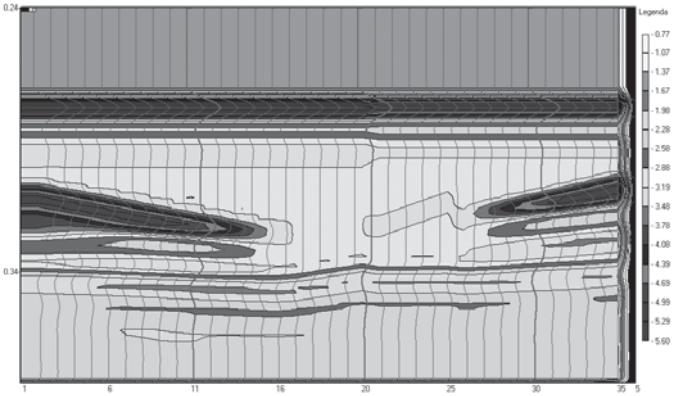

Fig. 4. Synthetic pseudo-impedance acoustic section for simplified seismological model I, f_0 = 60Hz, f_0/β = 1. Left Vertical axe: time in seconds, horizontal axe: number of traces, right axe: relative velocity in km/s displayed as colour scale

The synthetic pseudoimpedance acoustics section generated for long signal duration time f_0/β = 2 is presented in figure 5. The synthetic pseudoimpedance acoustics section generated for long signal duration time f_0/β = 2 and with predictive deconvolution applied before process inversion are presented in figure 6.

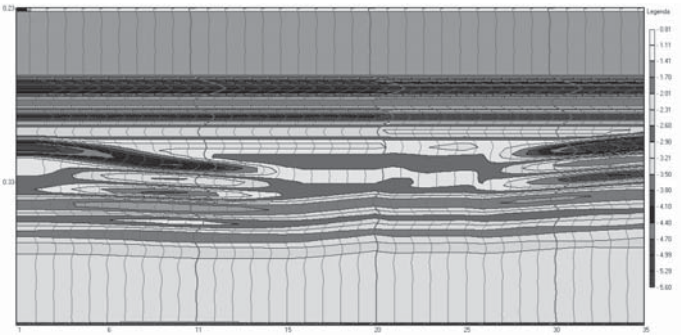

Fig. 5. Synthetic pseudo-impedance acoustic section for simplified seismological model I, f_0 = 60Hz, f_0/β = 2. Left Vertical axe: time in seconds, horizontal axe: number of traces, right axe: relative velocity in km/s displayed as colour scale

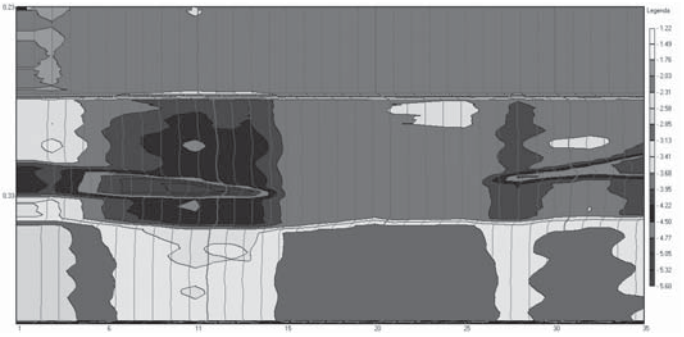

Fig. 6. Synthetic pseudo-impedance acoustic section for simplified seismological model I, f_0 = 60Hz, f_0/β = 2, deconvolution. Left Vertical axe: time in seconds, horizontal axe: number of traces, right axe: relative velocity in km/s displayed as colour scale

The presence of anhydrites is poorly visible for long signal, but an improvement of the resolution is possible for short signal. On the synthetic pseudoimpedance acoustics section generated with predictive deconvolution applied before the inversion process the contours are clearly visible.

The synthetic pseudoimpedance acoustics section presented in figures 7, 8, 9 are generated for simplified model II presented in figure 2. The section are generated for dominant frequency f_0 = 60Hz. The synthetic pseudoimpedance acoustics section generated for short signal duration time f_0/β = 1 (f_0 — dominant frequency, β — dumping factor), is presented in figure 7.

The synthetic pseudoimpedance acoustics section generated for long signal duration time f_0/β = 1 (f_0 — dominant frequency, β — dumping factor), is presented in figure 8.

On pseudoimpedance acoustic section generated for a long seismic signal the lens of anhydrite is visible, but is contour recognition impossible as is the estimation of the lense size. For a short seismic signal the resolution increases, when the predictive deconvolution is applied before process inversion the contours clearly visible. The synthetic pseudoimpedance

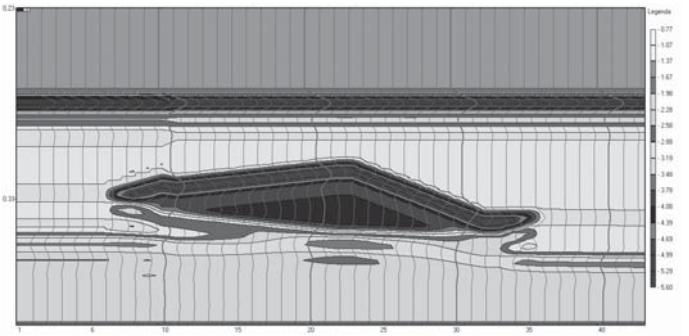

Fig. 7. Synthetic pseudo-impedance acoustic section for simplified seismological model II, f_0 = 60Hz, f_0/β = 1. Left Vertical axe: time in seconds, horizontal axe: number of traces, right axe: relative velocity in km/s displayed as colour scale

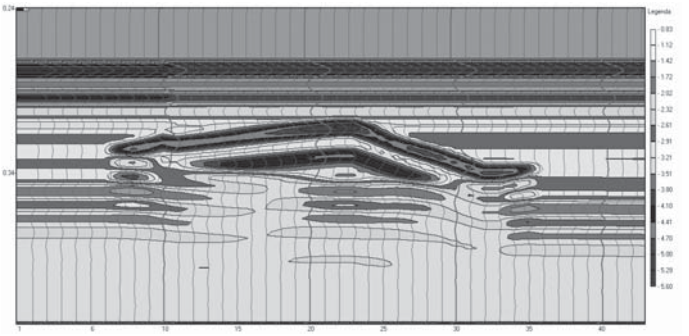

Fig. 8. Synthetic pseudo-impedance acoustic section for simplified seismological model I, f_0 = 60Hz, f_0/β = 2. Left Vertical axe: time in seconds, horizontal axe: number of traces, right axe: relative velocity in km/s displayed as colour scale

acoustics section generated for long signal duration time $f_0/\beta = 1$ (f_0 — dominant frequency, β — dumping factor), with predictive deconvolution applied before process inversion are presented in figure 9.

The synthetic pseudoimpedance acoustics section presented in figures 10, 11 and 12 are generated for a simplified model III presented on figure 3. The sections are generated for dominant frequency f_0 = 60 Hz. The synthetic pseudoimpedance acoustics section generated for short signal duration time $f_0/\beta = 1$ (f_0 — dominant frequency, β — dumping factor), is presented in figure 10.

The synthetic pseudoimpedance acoustics section generated for long signal duration time $f_0/\beta = 1$ (f_0 — dominant frequency, β — dumping factor), is presented in figure 11.

The synthetic pseudoimpedance acoustics section generated for long signal duration time $f_0/\beta = 1$ (f_0 — dominant frequency, β — dumping factor), with predictive deconvolution applied before the process of inversion is presented in figure 12.

The low size of the anhydrites lenses could be detected but the estimation of size and their contours is rather difficult. The resolution increases with the improvement of seismic

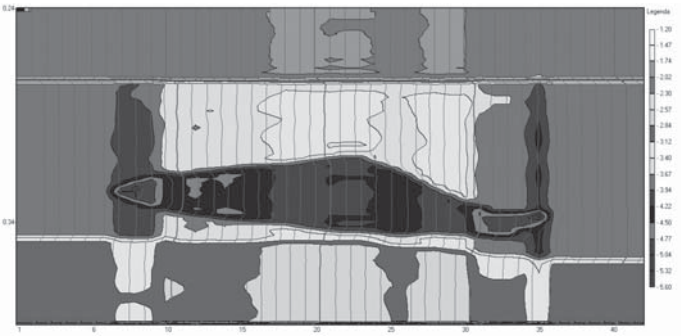

Fig. 9. Synthetic pseudo-impedance acoustic section for simplified seismological model II, f_0 = 60Hz, f_0/β = 2, deconvolution. Left Vertical axe: time in seconds, horizontal axe: number of traces, right axe: relative velocity in km/s displayed as colour scale

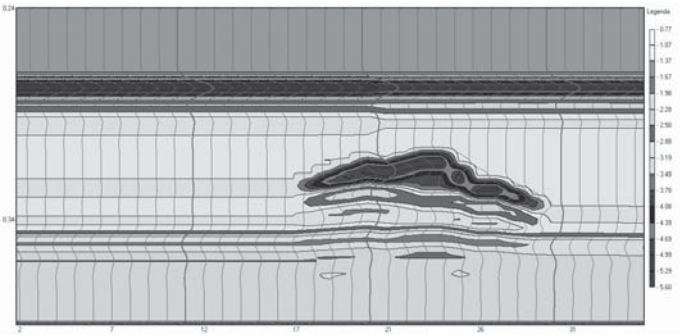

Fig. 10. Synthetic pseudo-impedance acoustic section for simplified seismological model III, f_0 = 60Hz, f_0/β = 1. Left Vertical axe: time in seconds, horizontal axe: number of traces, right axe: relative velocity in km/s displayed as colour scale

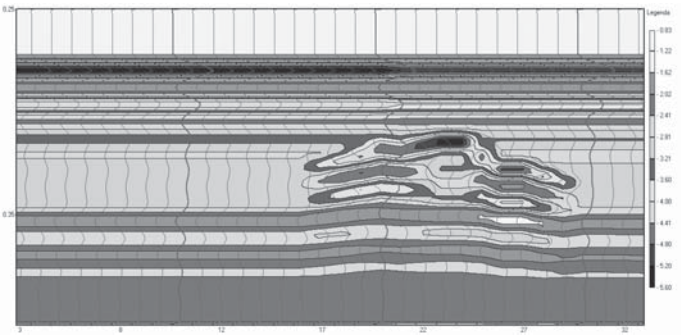

Fig. 11. Synthetic pseudo-impedance acoustic section for simplified seismological model III, f_0 = 60Hz, f_0/β = 1. Left Vertical axe: time in seconds, horizontal axe: number of traces, right axe: relative velocity in km/s displayed as colour scale

signal quality [2]. In practice the data is distorted by noise and wave propagation phenomena, which decreases reliability of interpretation [1].

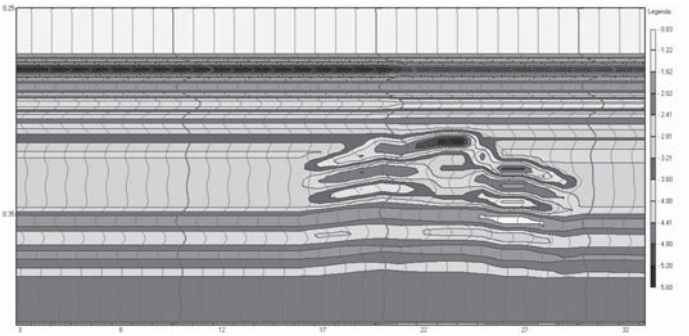

Fig. 12. Synthetic pseudo-impedance acoustic section for simplified seismological model III, f_0 = 60Hz, f_0/β = 1, deconvolution. Left Vertical axe: time in seconds, horizontal axe: number of traces, right axe: relative velocity in km/s displayed as colour scale

The synthetic pseudoimpedance acoustics section generated with predictive deconvolution applied before the process inversion was presented in figures. 6, 9 and 12 was generated for long signal duration time $f_0/\beta = 1$ (f_0 — dominant frequency, β — dumping factor). The application of predictive deconvolution before inversion of synthetic pseudoimpedance acoustics sections generated for short signal duration time provides also improve resolution, but the results are not so spectacular.

3. Summary

These modeled sections of synthetic pseudoacoustic impedance for salt deposit show how changes of thickness, shape and lithology can be visible on such a transformation of seismic sections. Internal structure of the salt deposit displays several lithological types of rock salt (pure coarse-crystalline salt, salt intercalated with anhydrite). Inversion increases the resolution of conventional seismic. In practice the reverse process is difficult, since it requires inversion of a low grade, the seismic trace, which is always distorted by noise and wave propagation phenomena. Modern seismic field data can be processed to eliminate much of the distortion. An important procedure to help repair the damage to the spectrum is deconvolution. Presented works give the positive answer about the possibility of predicting the inhomogeneities due to anhydrite salt in rock salts deposits. Pseudoimpedance sections can serve very well to map geologic structure and homogeneity control of large parts of deposit important for construction of underground reservoirs.

The work was supported by Geophysics Dept. AGH UST project (no. 11.11.140.769).

REFERENCES

[1] Kawalec-Latała E.: *Wpływ poziomu szumu na rozdzielczość sekcji pseudoimpedancji akustycznej w NW części LGOM*. Górnictwo Odkrywkowe 7/2007, p. 81–86.

[2] Kawalec-Latała E.: *The Influence of Seismic Wavelet on the Resolution of Pseudoimpedance Section for Construction of Underground Storage*. [Wpływ sygnału sejsmicznego na rozdzielczość sekcji pseudoimpedancji akustycznej w rejonie budowy podziemnych magazynów]. Gospodarka Surowcami Mineralnymi. Mineral Resources Management t. 24, z. 2/3, 2008, p. 387–397.
[3] Kawalec E.: *Inwersja sejsmiczna w rozpoznawaniu niejednorodności złóż soli perspektywicznych dla budowy podziemnych zbiorników*. Wydawnictwa AGH Kraków, seria: Rozprawy Monografie nr 201, 2009.
[4] Pieńkowski G., Wagner R.: *Magazynowanie węglowodorów w strukturach solnych PROJECT NATO — CCMS — oferta dla Polski, Europy i NATO*. Konferencja Paliwowo-Naftowa, Uniwersytet Warszawski, 22–23 marca 2006.
[5] Pushch R.: *Geological Storage of Radioactive Waste*. Springer 2008.
[6] Ślizowski R.: *Możliwości zagospodarowania podziemnych złóż i struktur solnych w Polsce na składowisko odpadów promieniotwórczych*. Przegląd Geologiczny, 54, 2006, s. 314.
[7] Veeken P.C.H., Da Silva M.: *Seismic Inversion Methods and Some of Their Constraints*. First break, vol. 22, 2004.